The AVO Template: a tool for AVO interpretation

James H. Crane, Gulf Coast 3-D; James M. Crane, Chevron U.S.A.; Juan M. Lorenzo, Louisiana State University*

Summary

Since the mid 1980's, amplitude versus offset (AVO) data have been used by earth scientists to help in the prediction of lithology using seismic data. Although previous work has greatly aided in our ability to interpret AVO data, the AVO response cannot be easily visualized with respect to changes in rock properties, lithology, porosity, fluid type, and fluid saturation utilizing available techniques. The "AVO Template" we introduce allows for this visualization. The AVO Template is a graphical display that predicts the AVO responses at a lithologic interface using rock properties and Shuey's parabolic approximation to Zoeppritz equations. The AVO Template allows an interpreter to visualize the changes in AVO response caused by changes in rock properties. In conjunction with a Rock Physics Template, the AVO Template can also be used to help estimate fluid type, porosity, and fluid saturation. Given the proper choice of parameters, the AVO Template can be used to help predict the probability of hydrocarbons in a prospective reservoir. Possible applications of the AVO Template include conventional and unconventional exploration and production, 4D seismic interpretation, and other applications where seismic data are used to predict lithology.

Introduction

The calculation of reflection coefficients has a long history (e.g., Knott, 1899, Zoeppritz, 1919, Muskat and Meres, 1940, Koefoed, 1955; Ewing et al., 1957, Tooley et al.,1965, Bortfeld, 1961, Aki and Richards, 1980), but the application of this body of scientific work to oil and gas exploration was delayed by the lack of Poisson's ratio measurements on relevant lithologies and the absence of long offset seismic data. Ostrander (1984) first applies reflection coefficient work to help identify gas sands. The Poisson's ratio of a brine-filled reservoir decreases as hydrocarbons are introduced. This reduction in Poisson's ratio affects the AVO response and therefore is the key for using AVO to predict hydrocarbon lithologies. Some of the contributions from the geophysical community that aid in AVO interpretation include theoretical work describing the P-wave reflection at an interface between two lithologies (Shuey, 1985), measuring rock properties for relevant lithologies (Mavko et al., 2009), modeling (Sherwood et al., 1983), crossplotting the measured AVO response (Castagna and Swan, 1997), and classification of various AVO responses (Rutherford and Williams, 1989). Although previous work has greatly aided in our ability to interpret AVO data, the AVO response cannot be easily visualized with respect to changes in rock properties, lithology, porosity, fluid type, and fluid saturation utilizing available techniques. Shuey (1985) presents a simplification of Zoeppritz equations (Zoeppritz, 1919) which has been widely used in the oil and gas industry (Castagna and Swan, 1997). Shuey derives a parabolic (two-term) approximation for the compressional wave reflection coefficient which is dependent on the change in density (ρ), P-wave velocity (Vp), and Poisson's ratio (σ) across a reflecting interface between two lithologies.

The "AVO Template" is a graphical display that uses Shuey's parabolic approximation to predict an infinite number of AVO responses from lithologies below a lithologic interface given the fixed rock properties of the upper lithology. The AVO Template (AVOT) allows an interpreter to visualize the changes in AVO response caused by changes in rock properties. Odegaard and Avseth (2003) introduced the concept of a Rock Physics Template (RPT) which uses rock physics along with mineral and fluid properties to predict Vp/Vs and acoustic impedance for various lithologies and fluid saturations. These RPT displays can be mapped on to the AVO Template by converting Vp/Vs values into Poisson's ratio values (Sheriff, 1973). In combination with a Rock Physics Template, the AVO Template allows an interpreter to visualize changes in the AVO response caused by changes in lithology, porosity, fluid type, and fluid saturation. The AVOT can be used to evaluate and illustrate a number of lithologic scenarios on the same display.

Methods

For the AVO Template, the AVO responses of the lower lithology (Lithology 2) are predicted using Shuey's parabolic equation given the fixed rock properties (ρ_1, Vp_1, σ_1) of the upper lithology (Lithology 1). While the rock properties of Lithology 1 are fixed, the rock properties (ρ_2, Vp_2, σ_2) of Lithology 2 vary across the template so an interpreter can evaluate the AVO responses of a number of different possibilities for Lithology 2 on the same display.

While Lithology 1 can be chosen to be any lithology, it might be useful to choose it to be the dominant lithology in the area of interest based on regional stratigraphy. For example, in a

shale-dominated basin, Lithology 1 could be chosen to be a shale. This shale, at a given depth interval, would have fairly constant rock properties (Castagna et al.,1985). The interval below this shale (Lithology 2) could be a sandstone whose rock properties change with porosity, fluid type, and fluid saturation. The AVO Template could then be used to evaluate the probability of hydrocarbons in that prospective sandstone reservoir by comparing a range of predicted hydrocarbon AVO responses to that observed in the properly processed seismic data (Graul and Hilterman, 2019).

Shuey (1985) evaluates the reflection coefficient at an interface between two lithologies. The compressional wave reflection coefficient, $R(\Theta_i)$, is given by

$$R(\Theta_i) = R_0 + R_0 A \Theta_i^2 \quad (1)$$

(Shuey, 1985; eq. 18) where Θ_i is the incident angle in radians, R_0 is the reflection coefficient at $\Theta_i = 0$, and A is a parameter that is informative of the contrast in Poisson's ratio between Lithology 1 and 2. Inspection of equation (1) reveals that the AVO response at a lithologic interface can be completely described by R_0 and the parabolic gradient, $M = R_0 A$. Since the AVOT is based on Shuey's parabolic approximation, it has the same limitations as described by Shuey (1985). The main limitation is the restriction to incident angles from 0 to 30 degrees.

There are two versions of the AVO Template. The three-parameter version (Figure 1) uses fixed rock properties (ρ_1, Vp_1, σ_1) from the upper lithology (Lithology 1) to predict the AVO responses of the lower lithology (Lithology 2). The three-parameter AVOT separates the AVO response into four volumes by creating a Zero Intercept Surface and a Zero Gradient Surface using the equations in Shuey (1985). The Zero Intercept Surface is created by choosing rock properties for the lower lithology (Lithology 2) which cause R_0 to be zero. The Zero Gradient Surface is created by choosing rock properties for the lower lithology (Lithology 2) which cause the parabolic gradient, M, to be zero.

The second version of AVOT (Figures 2 and 3) is a simplified, easier to use, two-parameter version which uses (Z_1, σ_1) values from Lithology 1 to predict the AVO responses of Lithology 2. Here Z_1 (Dobrin,1960) is the acoustic impedance of Lithology 1 given by $Z_1 = \rho_1 Vp_1$. This two-parameter AVOT separates the AVO response into four areas by creating a Zero Intercept Line and a Zero Gradient Contour using equations from Shuey (1985) and assuming a constant value for Shuey (1985) parameter B. The Zero Intercept Line is created by choosing rock properties for the lower lithology (Lithology 2) which cause R_0 to be zero. The Zero Gradient Contour is created by choosing rock properties for the lower lithology (Lithology 2) which cause the parabolic gradient, M, to be zero.

The major concept behind the AVOT methodology is to divide the (ρ, Vp, σ) volume (or the (Z, σ) plane) into four volumes (or areas) of distinctly different AVO character. The position of the rock property values of Lithology 2 predicts the AVO response. While the three-parameter AVOT gives a better prediction of the parabolic gradient, the two-parameter AVOT might be preferred because of the ease of calculation and display.

Three-Parameter AVOT

For demonstration purposes, Gulf Coast shale properties are used for Lithology 1 in the AVOT of Figure 1 (ρ_1=2.45 g/cc, Vp_1=3048 m/s, and σ_1=0.352). The Zero Intercept Surface is constructed so that any (ρ_2, Vp_2, σ_2) value for Lithology 2 which lies on this surface will have zero amplitude at zero incident angle (Figure 1). Lithology 2 values with Z_2 greater than Z_1 will have an AVO response that is positive at zero incident angle (R_0>0). Lithology 2 values with Z_2 less than Z_1 will have an AVO response that is negative at zero incident angle (R_0<0). The distance that a Lithology 2 (ρ_2, Vp_2, σ_2) value is from the Zero Intercept Surface indicates the magnitude of R_0. Figure 1 shows that this Zero Intercept Surface separates the (ρ, Vp, σ) space into two volumes. In one volume, the AVO response at the interface between Lithology 1 and 2 is positive at zero incident angle (R_0>0) and in the other volume the AVO response is negative at zero incident angle (R_0<0).

The Zero Gradient Surface is created by setting the parabolic gradient, $M = R_0 A$, in Shuey (1985), equal to zero and solving for σ_2. The resulting Zero Gradient Surface is shown in Figure 1. Any Lithology 2 whose (ρ_2, Vp_2, σ_2) value lies on this surface will have an AVO response with no increase or decrease in amplitude with increasing incident angle (zero gradient). Any Lithology 2 whose (ρ_2, Vp_2, σ_2) value lies above this surface (higher σ_2 values) will have an AVO response that becomes more positive with increasing incident angle (positive gradient). Any Lithology 2 whose (ρ_2, Vp_2, σ_2) value lies below this surface (lower σ_2 values) will have an AVO response that becomes more negative with increasing incident angle (negative gradient). The distance that a Lithology 2 (ρ_2, Vp_2, σ_2) value is from the Zero Gradient Surface indicates the magnitude of the parabolic gradient. The Zero Gradient Surface divides the (ρ, Vp, σ) space into two volumes, one with positive and one with negative gradient. The combination of the Zero Intercept Surface and the Zero Gradient Surface divides the (ρ, Vp, σ) space into four volumes, each with its own distinctive AVO character (Figure 1).

10.1190/segam2020-3409444.1

The AVO Template

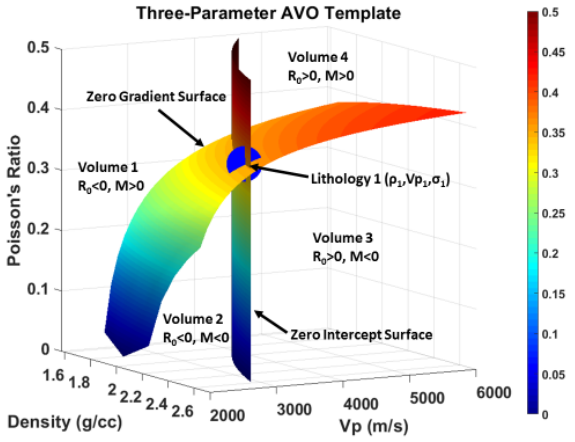

Figure 1. The rock properties for Lithology 1 (ρ_1=2.45 g/cc, Vp_1=3048 m/s, and σ_1=0.352) are used to create this three-parameter AVOT. The Lithology 1 rock properties are represented by a point at the center of the blue sphere. The Zero Gradient Surface and the Zero Intercept Surface are shown using the rainbow color scheme. Volume 1 is characterized by R_0<0 and M>0. Volume 2 has R_0<0 and M<0. Volume 3 has R_0>0 and M<0 while Volume 4 is characterized by R_0>0 and M>0. The AVO responses for any Lithology 2 change as the rock properties (ρ_2, Vp_2, σ_2) vary across the (ρ,Vp, σ) volume.

Two-Parameter AVOT

If an assumption is made about the value of the Shuey (1985) parameter B, the rest of the Shuey equation can be expressed in terms of Z and σ, which allow the two-parameter AVOT to be created. This assumption introduces an error in the prediction of the various parabolic gradients of the lower lithologies, but in most cases this error is small. This error becomes significant only at high values of R_0(1-2E) where $E = (1 - 2\sigma)/(1 - \sigma)$. Shuey (1985) demonstrates that when $\sigma = 1/3$ there is no variation in parabolic gradient, M, for changes in the parameter B.

If the assumption of $B = 0.8$ is used (Shuey, 1985, Appedndix A), the three-parameter AVO Template shown in Figure 1 can be simplified to a crossplot on the (Z, σ) plane. Using the same assumptions for Lithology 1 as in Figure 1 and assuming $B = 0.8$, the two-parameter AVO Template shown in Figure 2 can be constructed. Here the (Z,σ) plane is divided into four areas by the Zero Intercept Line and the Zero Gradient Contour.

The Zero Intercept Line is constructed by setting $R_0 = 0$ as shown by the gold line in Figure 2. The reflection from any Lithology 2 in the lower half space whose (Z_2, σ_2) value lies on this vertical line will have zero amplitude at zero incident angle. This line divides the (Z, σ) plane into two areas, one with R_0<0 and the other with R_0>0. The distance that a Lithology 2 (Z_2, σ_2) value is from the Zero Intercept Line indicates the magnitude of R_0.

The Zero Gradient Contour is constructed by setting the parabolic gradient, $M = R_0 A$, equal to zero. Assuming B=0.8, the Zero Gradient Contour, shown by the black contour in Figure 2, is created. Any Lithology 2 whose (Z_2, σ_2) value lies on this contour will have an AVO response with no change in amplitude with increasing incident angle. This contour divides the (Z, σ) plane into two areas, one with M<0 and the other with M>0. The distance that a Lithology 2 (Z_2, σ_2) value is from the Zero Gradient Contour indicates the magnitude of the parabolic gradient. The Zero Intercept Line and the Zero Gradient Contour combine to divide the (Z, σ) plane into four areas, each with a distinctive AVO response (Figure 2).

Figure 2 illustrates how the changes in AVO response that are caused by changes in rock properties can be visualized. For a constant Poisson's ratio of 0.25, the AVO response changes from Area 1 (R_0<0, M>0) to Area 2 (R_0<0, M<0) and finally to Area 3 (R_0>0, M<0) with increasing acoustic impedance (Z). For a constant Z of 8000 (g/cc x m/s) the AVO response changes from Area 3 (R_0>0, M<0) to Area 4 (R_0>0, M>0) with increasing Poisson's ratio. Both Rutherford and Williams (1989), and Castagna and Swan (1997) introduced AVO classifications of gas sands. Class 1 AVO reflections would be in AVO Template Area 3, Class 2 would be between Areas 2 and 3 near the Zero Intercept Line, Class 3 AVO would be included in Area 2, and Class 4 would be in Area 1. Although the three-parameter AVOT gives a more accurate prediction of the parabolic gradient, the two-parameter AVOT might be preferred because of the ease of calculation and display.

The AVO Template

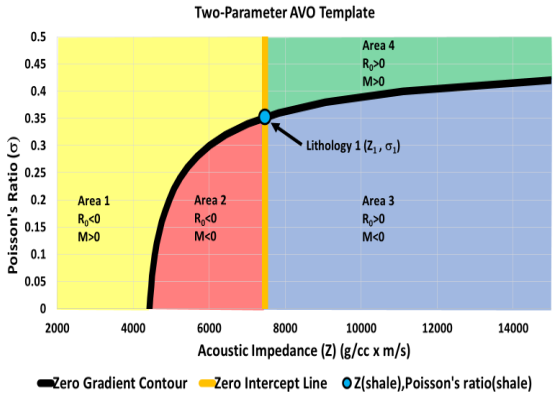

Figure 2. The two-parameter AVO Template resides on the acoustic impedance (Z), Poisson's ratio (σ) plane. The Lithology 1 rock properties are chosen to be Z_1=7468 (g/cc x m/s) and σ_1 = 0.352 which lie at the center of the blue dot. The gold vertical line represents the Zero Intercept Line. The AVO response from lower lithologies whose (Z, σ) values lie on this line have zero amplitude at zero incident angle. The black contour represents the Zero Gradient Contour. The AVO response from lower lithologies whose (Z, σ) values lie on this contour have no increase or decrease in amplitude with increasing incident angle. The Zero Intercept Line and the Zero Gradient Contour divide the (Z, σ) plane into four areas. Area 1 is characterized by R_0<0 and M>0. Area 2 has R_0<0 and M<0. In the same way, Area 3 has R_0>0 and M<0 while Area 4 is characterized by R_0>0 and M>0.

Rock Physics Template (RPT) Application

The RPT values taken from Figure 2 of Odegaard and Avseth (2003) are mapped on to an AVO Template (Figure 3). This figure illustrates how the AVO Template, in combination with a Rock Physics Template, allows an interpreter to visualize changes in AVO response beneath this 10% porosity shale caused by changes in lithology type, porosity, fluid content, and fluid saturation. As the lithology type changes from a 20% porosity shale to a 20% porosity brine sand, the AVO response changes from Area 1 (R_0<0, M>0) to Area 3 (R_0>0, M<0). The AVO responses for the different lithologies also change with porosity. For example, 40% porosity fully charged gas sands are in AVOT Area 1 (R_0<0, M>0), 37.5% to 17.5% fully charged gas sands are in Area 2 (R_0<0, M<0), and 15% to 10% fully charged gas sands are in Area 3 (R_0>0, M<0). In addition, the changes in AVO response owing to the fluid type and fluid saturation can be observed. As the gas saturation for a 20% porosity sand is increased, the Poisson's ratio and acoustic impedance for that sand are decreased. From Figure 3, the change in fluid type from 100% brine to 100% gas changes the AVO response from AVOT Area 3 (R_0>0, M<0) to Area 2 (R_0<0, M<0). The change in fluid saturation from 100% to 10% to 0% gas saturation causes a continuous change in AVO response from Area 2 to Area 3.

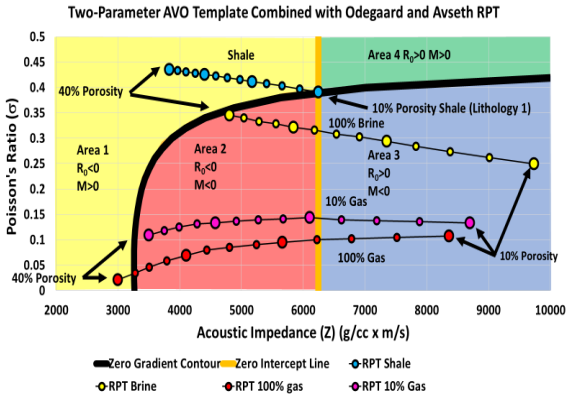

Figure 3. The Odegaard and Avseth (2003) RPT from Figure 2 of their paper is used to create this AVO Template. Lithology 1 for the AVOT is chosen to be the Odegaard and Avseth's RPT value for a 10% porosity shale. Porosities for shale, brine, 10% gas saturation, and 100% gas saturation are shown from 40% to 10% in 2.5% increments.

Conclusions

The AVO Template allows the interpreter to visualize the changes in AVO response caused by changes in rock properties. In combination with a Rock Physics Template, the AVO Template also allows the interpreter to visualize the changes in AVO response caused by changes in lithology, porosity, fluid type, and fluid saturation. In addition, the AVO Template allows the interpreter to compare the AVO response of a number of different lithologies on the same display.

Acknowledgements

I (JHC) would like to acknowledge the often underappreciated science and math educators. In my life those would include educators from Baton Rouge High, William Jewell College, Washington University in St. Louis, and the University of Houston. Also, I acknowledge my main clients, Badger Oil and Mack Energy, who keep me gainfully employed.

REFERENCES

Aki, K., and P. G. Richards, 1980, Quantitative seismology: W. H. Freeman and Co.

Castagna, J. P., M. L. Batzle, and R. L. Eastwood, 1985, Relationships between compressional-wave and shear-wave velocities in clastic silicate rocks: Geophysics, **50**, 571–581, doi: https://doi.org/10.1190/1.1441933.

Castagna, J. P., and H. W. Swan, 1997, Principles of AVO Crossplotting, The Leading Edge, **16**, 337–344, doi: https://doi.org/10.1190/1.1437626.

Dobrin, M. B., 1960, Introduction to geophysical prospecting: McGraw Hill.

Bortfeld, R., 1961, Approximation to the reflection and transmission coefficients of plane longitudinal and transverse waves: Geophysical Prospecting, **9**, 485–502, doi: https://doi.org/10.1111/j.1365-2478.1961.tb01670.x.

Ewing, W. M., W. S. Jardetzky, and F. Press, 1957, Elastic waves in layered media: McGraw-Hill.

Graul, M. and Hilterman, F., 2019, AVO: Seismic Lithology, SEG School Course Notes.

Knott, C. G., 1899, Reflection and refraction of elastic waves with seismological applications: Philosophical Magazine, **48**, 64–97, doi: https://doi.org/10.1080/14786449908621305.

Koefoed, O., 1955, On the effect of Poisson's ratio of rock strata on the reflection on coefficients of plane waves: Geophysical Prospecting, **3**, 381–387, doi: https://doi.org/10.1111/j.1365-2478.1955.tb01383.x.

Mavko, G., T. Mukerji, and J. Dvorkin, 2009, The rock physics handbook: Cambridge University Press.

Muskat, M., and M. W. Meres, 1940, Transmission and reflection coefficients for plane waves in elastic media: Geophysics, **5**, 149–155, doi: https://doi.org/10.1190/1.1441798.

Odegaard, E., and P. Avseth, 2003, Interpretation of elastic inversion results using rock physics templates: 65th EAGE Conference & Exhibition, Expanded Abstracts, doi: https://doi.org/10.3997/2214-4609-pdb.6.E17.

Ostrander, W. J., 1984, Plane-wave reflection coefficients for gas sands at nonnormal angles of incidence: Geophysics, **49**, 1637–1648, doi: https://doi.org/10.1190/1.1441571.

Rutherford, S. R., and R. H. Williams, 1989, Amplitude-versus-offset variations in gas sands: Geophysics, **54**, 680–688, doi: https://doi.org/10.1190/1.1442696.

Sheriff, R. E., 1973, Encyclopedic dictionary of exploration geophysics: SEG.

Sherwood, J. W. C., F. J. Hilterman, R. N. Neale, and K. C. Chen, 1983, Synthetic seismograms with offset for a layered elastic medium: Presented at 1983 Offshore Technology Conference.

Shuey, R. T., 1985, A simplification of the Zoeppritz equations: Geophysics, **50**, 609–614, doi: https://doi.org/10.1190/1.1441936.

Tooley, R. D., T. W. Spencer, and H. F. Sagoci, 1965, Reflections and transmission of plane compressional waves: Geophysics, **30**, 552–570, doi: https://doi.org/10.1190/1.1439622.

Zoeppritz, K., 1919, Erdbebenwellen VIII B, Uber Refexion and Durchgang seismischer Wellen durch Unstetigkritsflachen: Gottinger Nachr, **1**, 66–84.